2. Olmsted, P. D. & Goldbart, P. Isotropic-nematic transition in shear flow: state selection, coexistence, phase transitions, and critical behaviour. *Phys. Rev. A* **46**, 4966–4997 (1992).

3. Wang, X. J. & Warner, M. Theory of nematic comb-like polymers. *J. Phys. A* **20**, 713–731 (1987).

4. Noirez, L., Keller, P. & Cotton, J. P. On the structure and the chain conformation of side-chain liquid crystal polymer. *Liq. Cryst.* **18**, 129–148 (1995).

5. de Gennes, P. G. & Prost, J. *The Physics of Liquid Crystals* 2nd edn, 66, 164 (Clarendon, Oxford, 1993).

6. Noirez, L., Daoud-Aladine, A. & Boeffel, C. Scaling laws in side-chain liquid crystalline polymers. *Phys. Rev. Lett.* **80**, 1453–1456 (1998).

7. Fourmeaux-Demange, V., Boué, F., Brûlet, A., Keller, P. & Cotton, J. P. Effect of the molecular weight on the whole conformation of a liquid crystal comb-like polymer in its melt. *Macromolecules* **31**, 801–806 (1998).

8. Reys, V. *et al.* Short-range-order effects in the isotropic phase of a side-chain polymeric liquid crystal. *Phys. Rev. Lett.* **61**, 2340–2343 (1988).

9. Schmitt, V., Lequeux, F., Pousse, A. & Roux, D. Flow behavior and shear induced transition near an isotropic/nematic transition in equilibrium polymers. *Langmuir* **10**, 955–961 (1994).

10. Berret, J. F., Roux, D. C., Porte, G. & Linder, P. Shear induced isotropic to nematic phase transition in equilibrium polymers. *Europhys. Lett.* **25**, 521–526 (1994).

11. Mather, P. T., Romo-Uribe, A., Han, C. D. & Kim, S. S. Rheo-optical evidence of a flow induced isotropic-nematic transition in a thermotropic liquid crystalline polymer. *Macromolecules* **30**, 7977–7989 (1997).

12. Pleiner, H. & Brand, H. R. Local rotational degrees of freedom in nematic liquid-crystalline side-chain polymers. *Macromolecules* **25**, 895–901 (1992).

13. Rubin, S. F., Kannan, R. M., Kornfield, J. A. & Boeffel, C. Effect of mesophase order and molecular weight on the dynamics of nematic and smectic side-group liquid-crystal polymers. *Macromolecules* **28**, 3521–3530 (1995).

14. Cappellaere, E., Berret, J. F., Decruppe, J. P. & Linder, P. Rheology, birefringence and small-angle neutron scattering in a charged micellar system: evidence of a shear induced phase transition. *Phys. Rev. E* **56**, 1869–1878 (1997).

15. Gleim, W. & Finkelmann, H. Effect of the spacer length on the mechanical coupling between network and nematic order. *Makromol. Chem.* **192**, 2555–2579 (1991).

16. Gallani, J. L., Hilliou, L. & Martinoty, P. Abnormal viscoelastic behavior of side-chain liquid-crystal polymers. *Phys. Rev. Lett.* **72**, 2109–2112 (1994).

17. Brand, H. R. & Kawasaki, K. Mode coupling theory of the isotropic-nematic transition in side-chain liquid crystalline polymers. *J. Phys. II France* **4**, 543–548 (1994).

18. Noirez, L. & Lapp, A. Steady-state shear experiments on a side-chain liquid-crystal polymer: determination of the polymer conformation and liquid-crystal structure. *Phys. Rev. E* **53**, 6115–6120 (1996).

19. Noirez, L. Shear-induced S_A-S_C transition in side-chain liquid-crystalline polymers. *Phys. Rev. Lett.* **84**, 2164–2167 (2000).

20. Pieranski, P. & Guyon, E. Instability of certain flows in nematic liquids. *Phys. Rev. A* **9**, 404–417 (1974).

21. Dealy, J. H. & Wisbrun, K. *Melt Rheology and its Role in Plastics Processing* (Van Nostrand Reinhold, New York, 1990).

22. Finkelmann, H., Ringsdorf, H., Siol, W. & Wendorff, J. H. Model consideration and examples of enantiotropic liquid crystalline polymers. *Makromol. Chem* **179**, 273 (1978).

23. de Gemmes, P. G. *Scaling Concepts in Polymer Physics* 165, 224 (Cornell Univ. Press, 1979).

....

An abrupt climate event in a coupled ocean–atmosphere simulation without external forcing

Alex Hall* & **Ronald J. Stouffer**†

* *Lamont-Doherty Earth Observatory, Palisades, New York 10964, USA*
† *Geophysical Fluid Dynamics Laboratory, Princeton, New Jersey 08542, USA*

....

Temperature reconstructions from the North Atlantic region indicate frequent abrupt and severe climate fluctuations during the last glacial and Holocene periods[1-3]. The driving forces for these events are unclear and coupled atmosphere–ocean models of global circulation have only simulated such events by inserting large amounts of fresh water into the northern North Atlantic Ocean[4,5]. Here we report a drastic cooling event in a 15,000-yr simulation of global circulation with present-day climate conditions without the use of such external forcing. In our simulation, the annual average surface temperature near southern Greenland spontaneously fell 6–10 standard deviations below its mean value for a period of 30–40 yr. The event was triggered by a persistent northwesterly wind that transported large amounts of buoyant cold and fresh water into the northern North Atlantic Ocean. Oceanic convection shut down in response to this flow, concentrating the entire cooling of the northern North Atlantic by the colder atmosphere in the uppermost ocean layer. Given the similarity between our simulation and observed records of rapid cooling events, our results indicate that internal atmospheric variability alone could have generated the extreme climate disruptions in this region.

An extreme event is evident in the time series of surface air temperature (SAT) over southeastern Greenland and the neighbouring oceans (Figs 1a and c). Occurring around model year 3100, it lasts approximately 40 yr and is characterized by cooling of about 3 °C. As it is more than six standard deviations (σ) from the mean at its peak, the cooling can objectively be considered extreme. If the time series of annual mean SAT values in this region were normally distributed, such an anomaly would occur once every few hundred million years. Also, the probability that such a large cooling would last so long is extremely small. If the variations that last for less than 40 yr are removed from the time series, the SAT at the event's peak lies 10–11σ below the mean.

The source of this extraordinary lower-atmospheric cooling is a precipitous drop in underlying sea surface temperature (SST). Beginning around model year 3086, a modest cold SST anomaly of about 0.5 °C develops off central Greenland's east coast. This cooling intensifies until model year 3100, reaching 2.0–2.5 °C. Then it expands southwest along Greenland's entire east coast (Fig. 2a), reaching a peak magnitude of about 4.0 °C. The annual mean SST anomalies during this phase are 8–10σ below the mean. The evolution of sea surface salinity (SSS) anomalies is similar. At the event's peak (Fig. 2b), large amounts of fresh water appear along Greenland's entire southeastern coast. This SSS anomaly also lies 8–10σ below the mean.

These surface anomalies can be traced to an abnormally intense East Greenland current. Flowing southward along Greenland's east coast in the model as in reality[6], this current transports relatively cold and fresh Arctic water into the northern North Atlantic Ocean. At around model year 3083, the current gradually intensifies off central Greenland, leading to cooling and freshening there. Then, around model year 3096, the intensification expands, reaching Greenland's tip by year 3100 (Fig. 2d). This leads to the massive cooling and freshening along Greenland's southeast coast at the event's peak. By model year 3120, the current anomaly disappears.

The intensity of the East Greenland current at this stage is unusual, partly explaining the unusual drops in SST and SSS. Measured through the southward component of the surface current across the Denmark Strait (66.7° N, 13.1 to 28.1° W), the annual mean current intensity rises about 4.5σ above the mean. When variations of duration less than 40 yr are removed, the intensity is about 6σ above the mean, indicating that the current's strength is even more unusual when its long duration is taken into account.

Cooling and freshening off central Greenland's east coast and the intensification of the East Greenland current are characteristics of the model's 'great salinity anomalies' (GSAs)—a quasi-periodic 40–80-yr oscillation already documented in this model[7]. A typical simulated GSA involves a cooling of about 1–1.5 °C and freshening of about 0.2–0.3 practical salinity units, psu, off the central Greenland coast. This is broadly consistent with actual GSAs that occurred in the late 1960s and 1970s, and possibly also in the early part of the twentieth century[8]. Early in its lifetime, the extreme event resembles a typical simulated GSA. However, by model year 3101, it differs significantly in magnitude and in geographical extent (Figs 2a and

b). Whereas typical simulated GSAs are centred between Iceland and Greenland, the extreme event's SST and SSS anomalies extend from there to beyond the tip of Greenland.

Why is this GSA so extreme? The explanation lies partly in the reason for the unusually intense East Greenland current. Surface winds strengthen this current, transforming a typical GSA into the extreme event. The surface pressure anomaly pattern during the extreme event (Fig. 3) drives northwesterly winds along Greenland's east coast. These winds, in turn, induce a southwestward Ekman current in the surface ocean. In fact, the strongest northwesterly winds over Greenland's coast in the 15,000-yr experiment coincide exactly with the extreme event. (Figure 4 shows information on northwesterly wind index definition and data processing.) The winds begin intensifying around model year 3080, reaching values about $4-5\sigma$ above the mean at around year 3100. By year 3120, they subside. This strongly indicates that the unusually intense north-westerly winds are the trigger for the extreme event.

Other unusually large but less extreme GSAs occur in this experiment and are also linked to abnormally strong northwesterly winds. The SST variability distribution in the Denmark Strait (Fig. 4) reveals several instances of improbably cold SST but not correspondingly large warm events. Whereas no warm anomaly exceeds 3σ, the SST falls more than 3σ below the mean for a total of 163 yr, of which 33 yr are attributable to the extreme event. These represent a total of 10 separate events where the SST is unusually cold for several years at a time. During all these years, the north-westerly winds blowing across the Denmark Strait are stronger than normal. There is a less robust correspondence between more typical GSAs and wind strength. The correlation between the entire SST and wind strength time series is -0.55, but the correlation falls to -0.39 if times when SST fluctuations are greater than 1σ from the mean are removed from the two time series. Wind variations certainly generate highly unusual GSAs through their effect on surface currents, but they probably play a weaker role in more typical GSAs.
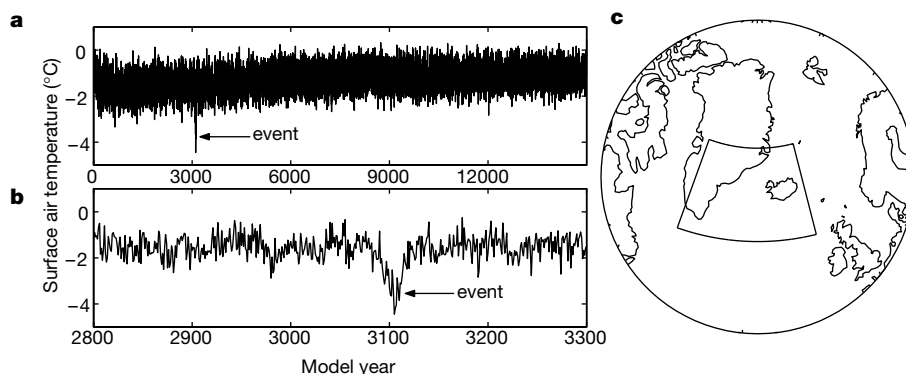

Figure 1 Time series of surface air temperature averaged over southeast Greenland and the neighbouring ocean (57.8−71.1° N, 11.3−48.8° W). **a**, Entire model integration; **b**, model years 2800−3300 only. **c**, The box encloses the region used for averaging in **a** and **b**.

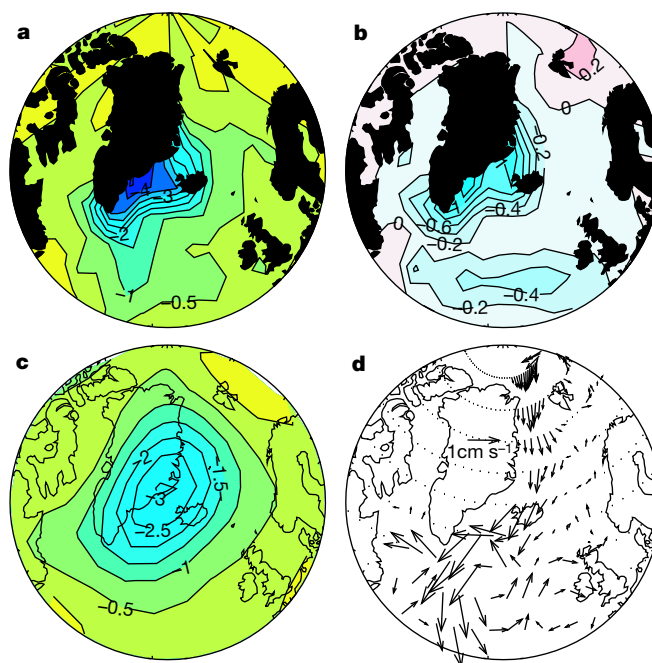**Figure 2** Sea surface temperature and salinity, surface air temperature and ocean current anomalies. **a**, SST (°C); **b**, SSS (practical salinity units or psu); **c**, SAT (°C); and **d**, surface ocean currents averaged over model years 3101−3110, the approximate decade when the event reaches its peak. All anomalies are calculated relative to the first 5,000 yr of the experiment. Real rather than model geography is used to facilitate orientation. A few hundred kilometres wide, the model's East Greenland current is qualitatively realistic, transporting on average about 4 sverdrups of Arctic water southward along Greenland's coast. However, due to the model's coarse resolution, the simulated current is wider and slower than the observed current, which transports about 8 sverdrups of water southward in a narrow coastal strip about 150 km wide[6].

SST in this region is very sensitive to northwesterly wind fluctuations when the winds are stronger than normal (Fig. 4). This is due to a climate instability unique to this region. The cold and fresh surface waters entering the area off Greenland's coast during unusual GSAs are very buoyant. During the extreme event, annual mean surface density, a function of temperature and salinity, falls $8-10\sigma$ below the mean in the area where SST and SSS are unusually low. Thus, the density-reducing effects of low SSS overwhelm the density-increasing effects of cold SST. Because of their extreme buoyancy, the cold, fresh waters eliminate deep convection off Greenland's southeastern coast. Like other high-latitude locations, the frigid atmosphere in this region constantly absorbs heat from the relatively warm ocean. The cutoff of surface waters from underlying layers during a convection shutdown sharply reduces the ocean's effective heat capacity. This concentrates the entire atmospheric cooling of the ocean in the first layer, amplifying the cold SST of invading northern waters. This positive feedback does not operate when northwesterly winds are unusually feeble, the East Greenland current weakens, and SST rises above normal (Fig. 4). Because SSS and hence surface density are also high at these times, convection may be enhanced; this does little, however, to alter the effective heat capacity of the ocean, because deep convection already exists here. This asymmetry explains why SST is affected to a much greater extent by wind-driven intensification rather than by weakening of the East Greenland current. This positive feedback would also operate if these waters became fresher because of a large meltwater discharge from ice sheets. In fact, much of this region's initial cooling in numerical experiments simulating such events[5] may be due to a convection shutdown.

This asymmetrical positive feedback explains how a merely unusual wind intensification produces a much more extreme variation in SST. The probability of finding a wind anomaly $4-5\sigma$ below the mean in a 15,000-yr normally distributed time series is not negligible. For example, we would expect an anomaly 4σ from the mean to occur approximately once every 7,500 yr. Moreover, the northwesterly wind index time series contains equal amounts of variability on all timescales longer than a few days. This suggests that wind variability in this region is randomly generated by the model atmosphere, rather than induced in some way by local SST variability, which has a spectral peak at the $40-80$-yr timescale. In addition, the low-frequency component of the model's North Atlantic Oscillation (NAO), an internal mode of the atmosphere, is positive during the entire extreme event (Fig. 4 has details on the NAO index). The NAO's positive phase is associated with abnormally strong westerly winds over the North Atlantic from $45-70°$ N. The unusual intensity of the northwesterly winds blowing across Greenland during the event thus stems partly from the positive NAO. For these reasons, the wind fluctuation that triggers the extreme event probably results from the model atmosphere's internal variability.

This unusual wind fluctuation affects the climate elsewhere by moving warm maritime air over the Eurasian continent. This causes a widespread SAT increase of about $0.5°$C over Europe and
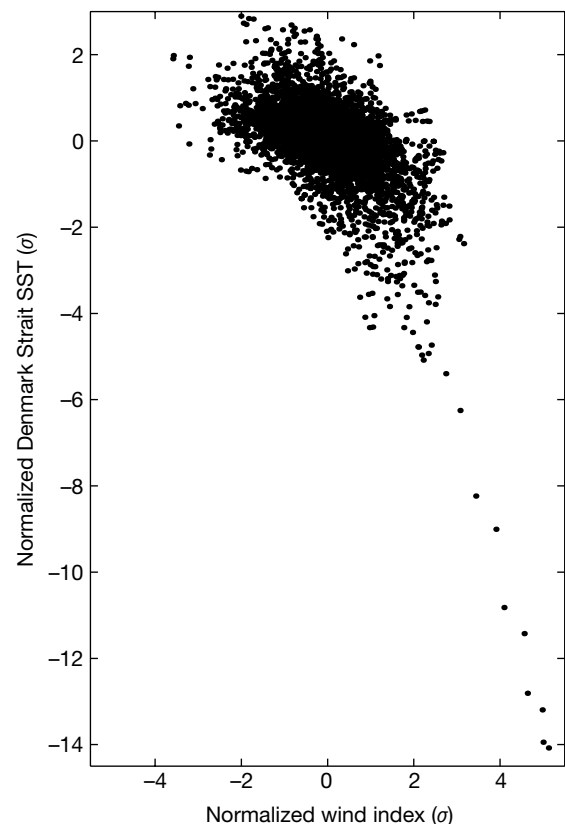
Figure 4 Scatter plot of sea surface temperature (SST) averaged over the Denmark Strait ($62.2-66.7°$ N, $18.8-30°$ W) versus winds blowing perpendicular to the Denmark Strait. Before plotting, SST was made to lag the wind index by 2 yr. The ten points representing the coldest SSTs all correspond to the extreme event. The wind index is defined as the surface pressure difference between two regions: $48.9-57.8°$ N, $33.8-56.25°$ W (an area south of the tip of Greenland) and $66.7-75.6°$ N, $11.3-41.3°$ E (centred over northern Scandinavia). A Hamming 40-yr low-pass filter has been applied to the SST and wind index, and both time series have been normalized by their respective standard deviations. For clarity, only every third year of the time series is shown. The model climate exhibits a quasi-linear millennial-scale trend over the course of the 15,000-yr experiment (Fig. 1a). To ensure this model drift does not distort the distribution of variability presented here, all variations lasting longer than 1,000 yr were removed from the SST and wind index time series using a Hamming high-pass filter. The North Atlantic Oscillation index is defined as the pressure difference between two regions: $40.0-48.9°$ N, $11.2-26.2°$ W and $66.7-75.6°$ N, $3.8-18.8°$ W). Variations lasting less than 40 yr were also removed from this time series.
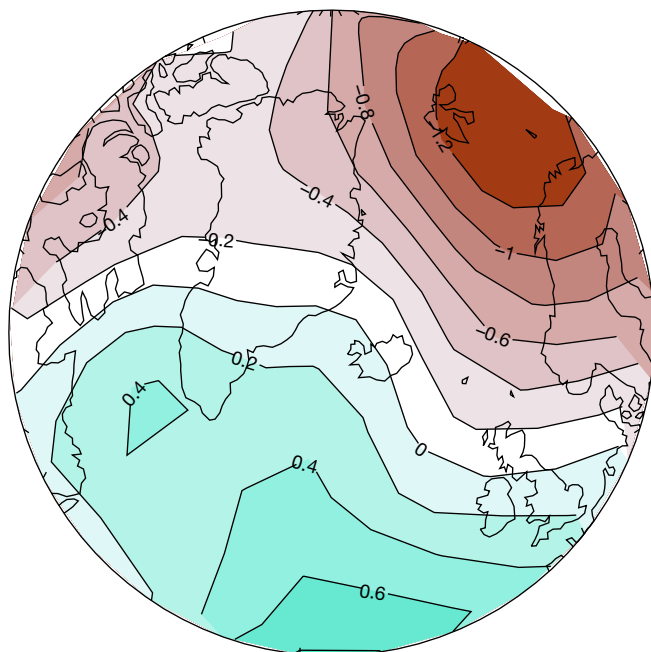

Figure 3 The surface pressure anomalies (in hPa) relative to the first 5,000 yr of the experiment averaged over model years 3096−3110. This pattern is typical of the surface pressure anomalies during most of the extreme event. As the simulated climatological winds over Greenland blow predominantly from the west, the winds driven by this pressure pattern represent both an increase in wind strength and a slight change in direction towards the south.

central Eurasia at the event's peak (model years 3101–3110). These temperatures are the warmest of the entire low-frequency (timescale ≥40 yr) time series of SAT averaged over this region, rising about 3.5σ above the mean. Although it is less extreme than the simultaneous cooling over southern Greenland (Fig. 2c), this warming covers a much wider area, so that the extreme event's signature is not visible in a hemispheric or global mean time series of SAT.

The simulated extreme event is qualitatively similar to some abrupt millennial-scale North Atlantic cooling events seen in the Holocene record[1]. The observed episodes, for which there is no known external forcing, are characterized by intensification of the East Greenland current, transport of water from the north of Iceland into the northern North Atlantic, and drops in SST of about 2 °C. In addition, the observed millennial-scale events have a signal in the low-latitude North Atlantic[9]. The simulated event also has a signal throughout the North Atlantic: the buoyant waters invading the northern North Atlantic slow the model's North Atlantic overturning, beginning around model year 3104. By year 3115, the thermohaline circulation weakens by about 16% from its mean value of 17.6 sverdrups (a 3.5σ anomaly). This reduces SST throughout the North Atlantic by a few tenths of a degree. Because the thermohaline circulation weakening occurs well after the event's onset, it is a response to the event rather than its cause.

The real millennial-scale events differ from the simulated event in that they probably last somewhat longer than 30–40 yr, although their exact length is uncertain since the marine sediments supplying information about them are subject to bioturbation. They also recur roughly every 1,500 yr (ref. 1). The simulated extreme event only occurred once during the entire experiment, so similar events would probably be rarer than the observed events if the experiment were continued for longer than 15,000 yr. These differences could be attributable to a deficiency in the model—the coarse resolution of the ocean model forces us to use unrealistically high horizontal and vertical diffusivity[10,11]. This probably makes the North Atlantic climate more stable than it should be. The massive outflow of cold and fresh water during the extreme event diffuses too quickly into the surrounding warm salty water, shortening the event's lifetime and limiting its geographical extent. The other simulated cold events where Denmark Strait SST falls more than 3σ below the mean might have developed further, lasted longer, and covered a larger area if the model ocean were less diffusive. As we noted above, over the course of the 15,000-yr experiment there are ten such events.

Although the probability of this type of drastic event happening in the near future seems low, it may be increasing for two reasons. First, nearly all coupled ocean–atmosphere models show an increase in atmospheric fresh water transport to the Arctic of about a tenth of a sverdrup when atmospheric CO_2 is doubled[12]. This significantly freshens the Arctic. Because the mechanism for the extreme event relies on fresh water transport out of the Arctic, increasing greenhouse gas concentrations could make a similar event more likely. Second, consistent with the observed 20–30-yr increase in the real climate's NAO index is a strengthening of the northwesterly winds blowing perpendicular to the East Greenland current[13,14]. If these winds continue to strengthen, they could produce a drastic climate event in the northern North Atlantic. □

Methods

The coupled ocean–atmosphere model[15] has a global domain with realistic geography. It has been used to study global warming[15–18], climate variability[19,20] and palaeoclimate[4,5,21]. The atmospheric component has nine vertical levels, with horizontal distributions of variables represented by spherical harmonics and grid-point values[22] with 4.5° latitude by 7.5° longitude spacing. Sunshine varies seasonally, but not daily. Cloud cover is predicted on the basis of relative humidity. A land surface model computes surface fluxes of heat and water[23]. The ocean component[24] employs a finite-difference technique using a grid system with approximately 4.5° latitude by 3.8° longitude spacing. There are 12 vertical levels in the ocean. The effects of mesoscale eddies are represented by diffusion of potential

temperature and salinity on constant-density surfaces. A sea-ice model computes ice thickness on the basis of thermodynamic heat balance and movement of ice by ocean currents. The atmospheric and oceanic components exchange heat, water, and momentum once a day. The 15,000-yr experiment is designed to be a perpetual simulation of the present-day climate. Accordingly, carbon dioxide, the only greenhouse gas other than water vapour in the model, is fixed to present-day levels, and solar radiation does not vary from year to year. Continental ice sheets are fixed to their present-day positions. Glacial dynamics therefore play no role in the extreme event or any variability simulated by this model.

The coupled model's quasi-equilibrium initial condition is obtained by separate integrations of the atmospheric and oceanic components using observed surface boundary conditions (SST, SSS and sea-ice thickness). When the integration of the coupled model begins from this initial condition, the simulated climate drifts toward a less realistic equilibrium state. To reduce drift, the fluxes of heat and water at the ocean–atmosphere interface are adjusted by given amounts before they are imposed on the ocean surface. The flux adjustments are determined before the coupled model run from separate integrations of the atmosphere and ocean models. They do not change from one year to the next and are independent of the SST and SSS anomalies that develop during the simulation. Thus they neither damp nor amplify these anomalies in any systematic way. Although the adjustments do not eliminate the shortcomings of the model[25], they do help to prevent rapid drift from the initial state. Such drift could seriously distort the internal variability that is the subject of this study.

1. Bond, G. *et al.* A pervasive millennial-scale cycle in North Atlantic Holocene and glacial climates. *Science* **278,** 1257–1266 (1997).
2. Dansgaard, W. *et al.* A new Greenland deep ice core. *Science* **218,** 1273–1277 (1982).
3. Johnsen, S. J. *et al.* Irregular glacial interstadials recorded in a new Greenland ice core. *Nature* **359,** 311–313 (1992).
4. Manabe, S. & Stouffer, R. J. Simulation of abrupt climate change induced by freshwater input to the North Atlantic Ocean. *Nature* **378,** 165–167 (1995).
5. Manabe, S. & Stouffer, R. J. Coupled ocean-atmosphere model response to fresh-water input: Comparison to Younger Dryas event. *Paleoceanography* **12,** 321–336 (1997).
6. Woodgate, R. A., Fahrbach, E. & Rohardt, G. Structure and transports of the East Greenland Current at 75N from moored current meters. *J. Geophys. Res.* **104,** 18059–18072 (1999).
7. Delworth, T., Manabe, S. & Stouffer, R. J. Multidecadal climate variability in the Greenland Sea and surrounding regions: a coupled model simulation. *Geophys. Res. Lett.* **24,** 257–260 (1997).
8. Dickson, R. R., Meinke, J., Malmberg, S. A. & Lee, A. J. The "Great Salinity Anomaly" in the northern North Atlantic 1968–1982. *Prog. Oceanogr.* **20,** 103–151 (1988).
9. deMenocol, P., Ortiz, J., Guilderson, T. & Sarnthein, M. Coherent high and low latitude climate variability during the Holocene warm period. *Science* **288,** 2198–2202 (2000).
10. England, M. H. Using chlorofluorocarbons to assess ocean climate models. *Geophys. Res. Lett.* **22,** 3051–3054 (1995).
11. Rabitaille, D. Y. & Weaver, A. J. Validation of sub-grid-scale mixing schemes using CFCs in a global model. *Geophys. Res. Lett.* **22,** 2917–2920 (1995).
12. Kattenberg, A. *et al.* in *Climate Change 1995: The Science of Climate Change* 285–357 (Cambridge Univ. Press, Cambridge, 1996).
13. Hurrell, J. W. Decadal trends in the North Atlantic Oscillation regional temperatures and precipitation. *Science* **269,** 676–679 (1995).
14. Thompson, D. W. J., Wallace, J. M. & Hegerl, G. C. Annular modes in the extratropical circulation. Part II: trends. *J. Clim.* **13,** 1018–1036 (2000).
15. Manabe, S., Stouffer, R. J., Spelman, M. & Bryan, K. Transient responses of a coupled ocean-atmosphere model to gradual changes of atmospheric CO_2. Part I: annual-mean response. *J. Clim.* **4,** 785–817 (1991).
16. Manabe, S., Spelman, M. J. & Stouffer, R. J. Transient response of a coupled ocean-atmosphere model to gradual changes of atmospheric CO2. Part II: Seasonal response. *J. Clim.* **5,** 105–126 (1992).
17. Manabe, S. & Stouffer, R. J. Multiple-century response of a coupled ocean-atmosphere model to an increase of atmospheric carbon dioxide. *J. Clim.* **7,** 5–23 (1994).
18. Stouffer, R. J. & Manabe, S. Response of a coupled ocean-atmosphere model to increasing atmospheric carbon dioxide: Sensitivity to the rate of increase. *J. Clim.* **12,** 2224–2237 (1999).
19. Delworth, T., Manabe, S. & Stouffer, R. J. Interdecadal variation of the thermohaline circulation in a coupled ocean-atmosphere model. *J. Clim.* **6,** 1993–2011 (1993).
20. Manabe, S. & Stouffer, R. J. Low frequency variability of surface air temperature in a 1000-year integration of a coupled ocean-atmosphere model. *J. Clim.* **9,** 376–393 (1996).
21. Manabe, S. & Stouffer, R. J. Two stable equilibria of a coupled ocean-atmosphere model. *J. Clim.* **1,** 841–866 (1988).
22. Gordon, C. T. & Stern, W. A description of the GFDL Global Spectral Model. *Mon. Weath. Rev.* **110,** 625–644 (1982).
23. Manabe, S. Climate and the ocean circulation: I. The atmospheric circulation and the hydrology of the Earth's surface. *Mon. Weath. Rev.* **97,** 739–774 (1969).
24. Bryan, K. & Lewis, L. A water mass model of the world ocean. *J. Geophys. Res.* **84,** 2503–2517 (1979).
25. Marotzke, J. & Stone, P. Atmospheric transports, the thermohaline circulation, and flux adjustments in a simple coupled model. *J. Phys. Oceanogr.* **25,** 1350–1364 (1995).

Correspondence and requests for materials should be addressed to A.H. (e-mail: alexhall@ldeo.columbia.edu).